

Performance Evaluation and Development of Sustainable Pavement Surfaces Using Ultra-Thin Geopolymer Concrete Overlays



S. Rayapudi^{1*}, T. C. Rao²

¹Acharya Nagarjuna University, Guntur, India.

²Bapatla Engineering College, Bapatla, India.

ABSTRACT: This study investigates the viability of employing an ultra-thin Geopolymer Concrete (GPC) overlay, synthesized from ground granulated blast-furnace slag (GGBS) and fly ash (FA), as a sustainable white topping for asphalt pavements. The research emphasizes the stress-handling efficacy of GPC under load scenarios typical of low-volume road traffic. A finite element model (FEM) was meticulously developed using ABAQUS software to simulate the mechanical behaviour of a GPC ultra-thin white topping (UTWT) overlay applied over asphalt substrates. Key design variables, including overlay thickness, elastic modulus, and critical stresses induced by a 51 kN applied load, were systematically analysed. The FEM utilized a 1m x 1m panel configuration for the overlay system. Additionally, a non-linear regression model was formulated to predict critical corner stresses and enhance overlay design optimization. The findings demonstrate that the UTWT overlay effectively reduces stress concentrations and improves load distribution, substantiating its potential as a viable alternative to conventional cement concrete overlays. An increase in GPC layer thickness over asphalt foundations was observed to significantly attenuate critical stress magnitudes. This research positions GGBS-FA-based GPC as a sustainable and structurally proficient alternative for pavement rehabilitation, meeting performance requirements for low-volume roads while promoting long-term sustainability in pavement engineering.

KEYWORDS: Geopolymer concrete, Ultrathin white topping, Edge stress, Interface shear, FEM.

[Received Jan. 4, 2025; Revised April 28, 2025; Accepted May 10, 2025]

Print ISSN: 0189-9546 | Online ISSN: 2437-2110

I. INTRODUCTION

Transportation infrastructure is vital for socio-economic growth, connectivity and sustainable development, enabling efficient movement of people and goods. Among the common infrastructures, bituminous pavements are widely used but have limited durability, often experiencing issues like cracking and rutting due to repeated loads. Traditional maintenance solutions, such as bituminous overlays, though common, serve as temporary fixes requiring frequent maintenance to retain structural and functional integrity (Rasmussen & Rozycki, 2004). Concrete overlays though requiring a higher initial investment, have proven to be a cost-effective alternative due to their extended durability and lower maintenance needs. Geopolymer concrete overlays offer additional sustainability benefits, utilizing industrial by-products and reducing the carbon footprint compared to traditional concrete. Life cycle cost analyses (LCCA), which consider initial costs, maintenance, and vehicle operation expenses, suggest that traditional concrete pavements are more cost-effective over time than bituminous pavements (Jundhare & Khare, 2013). When evaluating geopolymer concrete pavements, LCCA

indicates potential for further cost savings and environmental advantages. Geopolymer concrete not only reduces carbon emissions but also offers comparable or superior durability. These characteristics lead to decreased maintenance frequency and overall life cycle costs, making geopolymer concrete a more sustainable and economical alternative (Turner and Collins, 2013).

One durable alternative is "white topping," a method that involves overlaying concrete onto existing bituminous surfaces to extend pavement life. The increasing demand for sustainable and durable pavement solutions has brought ultra-thin white topping (UTWT) into focus. White topping involves applying a concrete overlay on existing asphalt pavements to rehabilitate deteriorated surfaces and improve durability. This technique categorized into traditional white topping, thin white topping (TWT), and ultra-thin white topping (UTWT), based on the thickness of the concrete layer. UTWT, typically 50-100 mm thick, is a cost-effective, sustainable alternative for low to medium traffic roads. The bond between bituminous and concrete layers is commonly achieved by milling the bituminous pavement surface to a depth of 25 mm, as per IRC-SP-76 guidelines (IRC-SP-76, 2008). UTWT overlays have been applied to approximately 22 million square meters in the

*Corresponding author: samba1057@gmail.com

United States, proving their long-term reliability (Rasmussen & Rozycki, 2004). This success has led to UTWT adoption in other regions, including Europe and India. Rashmi et al. (2020) conducted an extensive performance evaluation of white topping layers over flexible pavements to improve their durability and sustainability. Their study focused on TWT and UTWT methods, using various concrete compositions, including plain cement concrete (PCC), GGBS, admixtures, and combinations. The research highlighted that a composite beam incorporating GGBS and admixtures demonstrated superior mechanical performance.

Rayapudi and Rao (2024) investigated the mechanical and impact resistance properties of fiber-reinforced GPC using fly ash and ground-granulated blast furnace slag as binders. The study demonstrated that the addition of steel fibers (0–2%) significantly enhanced the compressive, tensile, and flexural strengths of GPC. Impact resistance and energy absorption improved notably, with regression models accurately predicting performance trends. Numerical simulations validated the experimental results, indicating that fiber reinforcement reduced crack widths and improved toughness under impact loads.

Research has shown that incorporating supplementary cementitious materials (SCMs) like fly ash, ground granulated blast-furnace slag (GGBS), and silica fume in concrete overlays can enhance early strength and fatigue resistance, making UTWT a sustainable infrastructure solution (IRC-SP-76, 2008; Thomas, 2013). Rashad et al. (2014) investigated a high-volume fly ash blend with 10% silica fume and 10% slag, finding improved compressive strength and abrasion resistance across curing stages. Similarly, a 100 mm-thick bonded concrete overlay constructed in 2004 on a Canadian highway utilized fly ash and synthetic fibers, showing minor edge cracking but excellent long-term performance (Juhasz & Eng, 2015). An increase in the elastic modulus of underlying layers has been shown to reduce critical stresses at corners and interfaces, thereby improving structural performance. A 100-mm overlay with sustainable materials demonstrated superior performance under heavy loads (Krishna & Ch, 2023). The study highlighted that a thinner overlay (<100 mm) experiences increased shear stresses, necessitating robust bonding at the asphalt-concrete interface (NguyenDinh, 2023).

To model the complex load interactions and material behaviours within UTWT structures, finite element methods (FEM) are invaluable. Mechanistic-empirical design approaches that incorporate FEM allow for accurate calculations of stresses and strains within the pavement layers under applied loads. Initially, FEM analyses were limited to Kirchhoff's thin plate theory, but advancements in software like ABAQUS, DYNA-3D, LS-DYNA, EVERFE, JSLAB, and ANSYS have enabled 3D simulations of layered pavement systems, treating the subgrade as either a Winkler foundation or an elastic continuum (Mack et al., 1997). These models provide a detailed understanding of stress distributions, helping engineers to optimize overlay thickness and bonding requirements.

In another study, a 3D FEM was developed for UTWT overlay design, establishing design procedures and construction guidelines that have influenced modern UTWT applications. By incorporating variable stiffness to simulate bonding levels, this model accurately predicted strain distributions in the overlay (Mack et al., 1997). Subsequent studies have refined this approach further. Nishiyama et al. (2005) developed a 3D FEM with springs to simulate bonding quality between concrete and asphalt, validated against field strain data. To analyze potential overlay debonding, Mu and Vandenbossche (2007) created a cohesive zone model that examines the bonding interface between asphalt and concrete layers, addressing a critical component of UTWT performance and durability. Olita et al. (2020) provided recalibrated formulas for corner stress calculations, at corners using FEA in ANSYS, addressing the limitations of traditional models like Westergaard's Theory. Their study validated these formulas against experimental data, enabling more accurate stress predictions under varied loading scenarios. A study demonstrated that horizontal forces exacerbate shear stresses, contributing to debonding and rutting in UTWT layers (Honghui et al., 2020).

Analytical and finite element models continue to evolve, enhancing our understanding of fatigue and stress behaviours in UTWT overlays. Krishna and Ch (2022) used ANSYS software to simulate stress responses under varying loads, with a focus on sustainable materials in low-traffic applications. Their critical stress model demonstrated how material choices and bonding affect fatigue life, underscoring the need for secure bonds between overlay and substrate. Vandenbossche et al. (2017) developed a predictive model incorporating wheel load and temperature gradients, which are essential for minimizing longitudinal cracking in UTWT overlays. Research on UTWT for airports highlighted the importance of controlling size and thickness, recommending a maximum panel size of 1.8×1.8 m, a minimum thickness of 7 cm, and asphalt with an elastic modulus above 1,500 MPa (Zhu et al., 2019).

This research fills a significant gap by establishing a non-linear regression model based on FEM for UTWT overlays with an elastic foundation. Viewing the pavement layers as elastic solids, this approach predicts shear failure and surface stress effects more accurately. This study evaluates the performance of a double-blended GPC UTWT overlay on bituminous pavements, contributing to the body of knowledge on sustainable and resilient infrastructure.

II MATERIALS AND METHODS

Class F fly ash and ground granulated blast furnace slag are used as binders in the study, both conforming to ASTM C 618 F and ASTM C 1697-16 standards. Natural river sand was used as fine aggregate, while 20 mm and 12 mm-sized coarse aggregates met IS 383 standards and were tested as per IS 2386. The alkaline activator solution comprised 12M sodium hydroxide (NaOH) with 97–98% purity and sodium silicate (Na_2SiO_3) containing 14.7% Na_2O , 29.4% SiO_2 , and 55.9%

water by mass, with a 2.5:1 mass ratio of NaOH to Na₂SiO₃. Steel fibers, with a specific gravity of 7.85, tensile strength of 1.45 N/mm², 35 mm length, 0.5 mm diameter, and an aspect ratio of 70, were added in varying volumes (0%, 0.5%, 1%, 1.5%, and 2%) to enhance performance. Additionally, 8% water was incorporated by mass to optimize the workability of the geopolymer concrete mix. These materials were carefully selected to ensure compliance with standards and improve mechanical and durability characteristics (Rayapudi and Rao, 2024). The compressive and flexural strength of the M45-grade GPC white topping mix were 53MPa and 5.1MPa, respectively.

The GPC mix used in this study was developed to optimize strength. Key material properties such as elastic modulus, Poisson's ratio, and density, as shown in Table 1 were incorporated into the ABAQUS model. Westergaard's modified equations (Ioannides et al. 1999) were used to verify the finite element model (Samir et al., 2001).

$$\text{Interior Stresses: } \sigma_i = \frac{0.316 P}{h^2} \left[4 \log \left(\frac{l}{b} \right) + 1.069 \right] \quad (1)$$

where b is radius of equivalent distribution of pressure, b = a (when a/h > 1.724) or

$$b = \sqrt{1.6 a^2 + h^2} - 0.675h \quad (\text{when } a/h < 1.724)$$

$$\text{Corner Stresses: } \sigma_c = \frac{3 P}{h^2} \left[1 - \left(\frac{a\sqrt{2}}{l} \right)^{0.6} \right] \quad (2)$$

$$\text{Edge Stresses: } \sigma_e = \frac{0.803 P}{h^2} \left[4 \log \left(\frac{l}{a} \right) + 0.666 \left(\frac{a}{l} \right) - 0.034 \right] \quad (3)$$

where

$$l = \sqrt[4]{\frac{E_{gp} h^3}{12(1-\mu^2)k}} \quad \text{and} \quad a = \left(\frac{P}{\pi p} \right)^{0.5}$$

μ = Poisson's ratio of GPC,

E_{gp} = Modulus of elasticity of GPC (MPa),

P = Single Wheel Load (N), and p = Tyre pressure in MPa; 'l' = radius of relative stiffness, mm and 'a' = radius of the equivalent circular area, mm.

Shear stresses under Vertical Load:

Birman (1981) method explains how vertical shear stresses develop in thin concrete slabs UTWT when subjected to vertical wheel loads. These shear stresses arise due to the transfer of load through the depth of the concrete layer, especially at the interface with the asphalt layer underneath. The method provides a mathematical expression for calculating shear stress, τ_{zx} follows a parabolic pattern throughout the slab thickness as shown in Equation (4). The distribution is influenced by the transverse force $q(x)$, the static moment $S_y(z)$, and the moment of inertia I_y .

$$\tau_{zx} = \frac{q(x) S_y(z)}{I_y} \quad (4)$$

where a is radius and p is pressure, $q(x) = \frac{p a}{2}$,

$$I_y = \frac{i h_1}{1+\kappa\beta} \quad \text{and} \quad S_y(z) = z_c F$$

where

F is area calculated,

z_c is Centre coordination of F

Shear stress calculations were performed using an equivalent T-beam model, as proposed by Birman (1981). This model incorporates key parameters, including the thickness of the concrete layer h_c , the ratio of elastic moduli $\kappa = E_2/E_1$, and the layer thickness ratio $\beta = h_2/h_1$. The variables are described as follows

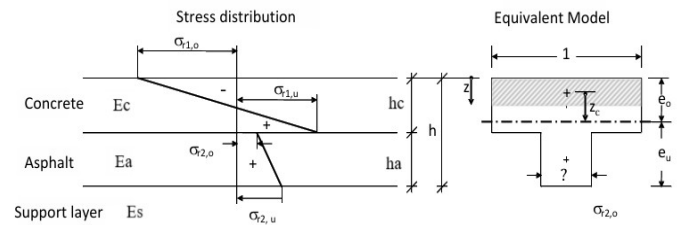


Figure 1: Stress Distribution and Equivalent Model for Composite Pavement System (NguyenDinh, 2023)

The main objective of Birman's method is to predict the vertical interface shear stress in a two-layer pavement system, quantify critical stress zones so that pavement designs include optimising the thickness of layers.

$$i = [1 + \kappa\beta(4 + 6\beta + 4\beta^2 + \kappa\beta^3)] \frac{h_1^2}{12} \quad (5)$$

$$e_0 = \frac{h_1(0.5 + \kappa\beta(1 + \frac{\beta}{2}))}{1 + \kappa\beta} \quad (6)$$

The shear flow at the base of the concrete layer, corresponding to $z = h_1$, was determined:

$$T(\kappa, \beta) = \frac{6(1+\beta)}{\frac{1}{\kappa\beta} + 4 + 6\beta + 4\beta^2 + \kappa\beta^3} \quad (7)$$

The maximum shear stress at the base of the concrete layer under a vertical load can be expressed as:

$$\tau_{zx} = p a \frac{T(\kappa, \beta)}{2 h_1 V} \quad (8)$$

$$v = \frac{a + e_0}{a}, \quad (9)$$

where 'v' is a factor that considers load distribution at a 45° angle to the neutral axis.

A. Finite Element Modelling

The 3D FEM for the UTWT pavement structure was modelled in ABAQUS (C3D8R-Element type) as a multi-layer pavement system comprising a geopolymer concrete

overlay, asphalt overlay, and subgrade in Figure 2. The overlay thickness was set to 80, 90, and 100 mm while the asphalt thickness was varied to 120, 110, and 100 mm such that the total thickness of the composite was 200mm. The subgrade was modelled as a Winkler foundation, with a modulus of subgrade reaction (k) of 0.148 MPa/mm accounting for the soil elastic behaviour. The overlay and asphalt layers were modelled with a planar dimension of 1 m x 1 m, suitable for analysing individual panels in pavement systems. The layer was discretized using 8-node hexahedral elements for accuracy in stress and displacement calculations. The mesh size was set to 30 mm, 8-noded brick element to balance computational efficiency and precision. A finer mesh resolution was applied near the loading zones to capture stress concentrations effectively. Contact interactions between the overlay and asphalt were defined with tie constraints to simulate perfect bonding conditions. A static wheel load of 51 kN was applied over a rectangular contact area of 200 mm x 150 mm, resulting in a uniform pressure of 0.85 MPa. The equivalent circular radius (a) for the contact area was calculated as 138 mm. Critical stresses computed at different load positions included Interior, Edge and Corner positions.

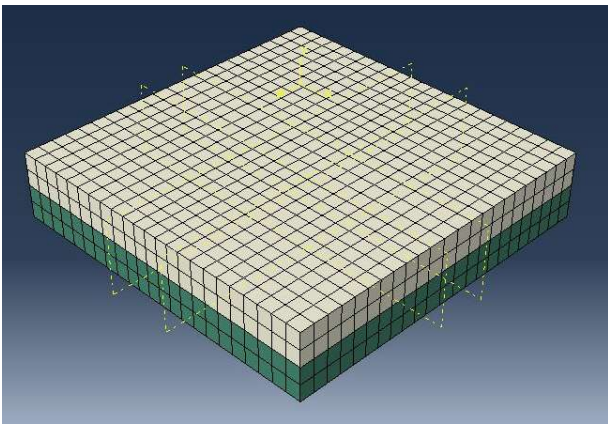


Figure 2: ABAQUS model with GPC White topping overlay on Asphalt concrete slab.

Boundary conditions were defined as the base of the subgrade layer was fixed to restrict vertical displacements. Horizontal displacements were permitted along the edges of the panel to simulate real pavement behaviour. Three critical loading positions were analysed at interior (centre of the panel), edge (along the boundary), and corner (at the intersection of two edges). The bottom of the subgrade was constrained to restrict vertical displacement, while horizontal movement was allowed along the edges to replicate realistic boundary conditions.

III PARAMETRIC STUDY ON THE FINITE ELEMENT MODELLING

A parametric study was conducted to evaluate how various factors influence the stress behaviour and structural performance of UTWT overlays. The study examined the impact of material properties and layer thickness variations. 3D

pavement is used as a linear 8-node solid model in FEM (Cheng 2006; Sheng et al. 2012). The mechanical properties of the pavement layers were selected based on guidelines from IRC-37 (2001) and recent studies on cement and geopolymer concrete. The geopolymer concrete overlay was modelled to exhibit compressive strengths equivalent to concrete grade M45 with corresponding elastic modulus. The geopolymer overlay thicknesses varied between 80 to 100 mm at an interval of 10mm.

In the ABAQUS 3D finite element model for analysing a 1 m x 1 m UTWT GPC overlay panel static loading, fixed constraints are applied to the bottom of the subgrade to restrict displacements in the X, Y, and Z directions. Horizontal constraints, restricting movement in the X and Z directions, are applied to the sides of the asphalt pavement layer, subbase, and subgrade to simulate realistic lateral confinement. The study primarily focused on determining the critical corner stress under varying conditions, as corner stress is a key parameter for assessing pavement durability. Perfect bonding was assumed between the geopolymer overlay and the asphalt layer. The contact between GPC UTWT and the Asphalt layer was fully continuous. The influence of overlay thickness, asphalt thickness, and material stiffness was analysed to identify optimal configurations that minimize stress concentrations and mitigate potential issues such as fatigue cracking, debonding and surface irregularities.

The parametric analysis offered insights into how layer properties and configurations affect pavement performance, providing a basis for designing durable UTWT systems that comply with guidelines like IRC-SP-76 (2008). By understanding the interaction between different parameters, the study supports the development of more robust and sustainable pavement systems.

Table 1: Material properties of Asphalt and Geopolymer Concrete

Layer	Thickness (mm)	Elastic Modulus (MPa)	Poisson's ratio	Density Kg/m ³
Geopolymer concrete	$h_c = 80, 90, 100$	$E_c = 32960$	$\nu_c = 0.15$	2400
Asphalt concrete	$h_a = 120, 110, 100$	$E_a = 1600$	$\nu_a = 0.35$	2324
Subbase	$h_b = 200$	$E_s = 150$	$\nu_b = 0.35$	1750

A. Corner, Edge and Interior Stresses

A. (i) Effect of ultra-thin white topping GPC layer thickness on Critical Corner Stress

The effect of critical corner stress and interface shear in the case of UTWT layer thickness of 80 mm, 90 mm, 100 mm and asphalt layer thickness of 120 mm, 110 mm, 100 mm with 1m panel size and $E_c = 32,960$ MPa. $E_b=1600$ MPa from the ABAQUS was assessed. Fig.3 shows ABAQUS figures for critical corner stress. Modelling showed that increasing the GPC thickness significantly improved performance.

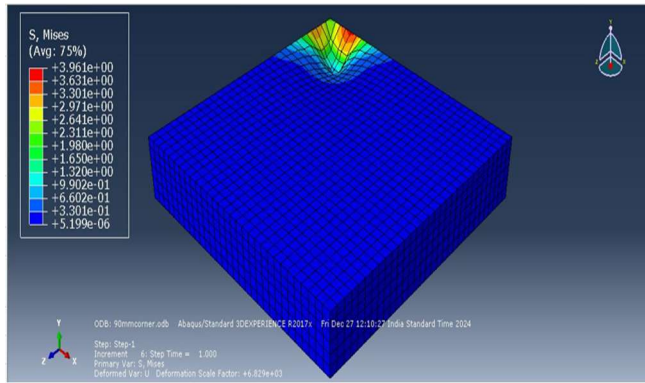


Figure 3: (a) Maximum critical corner stress for the 80 mm layer thickness of GPC UTWT

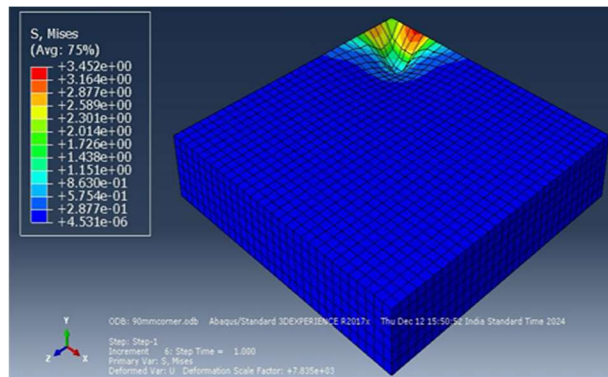


Figure 3: (b) Maximum critical corner stress for the 90 mm layer thickness of GPC UTWT

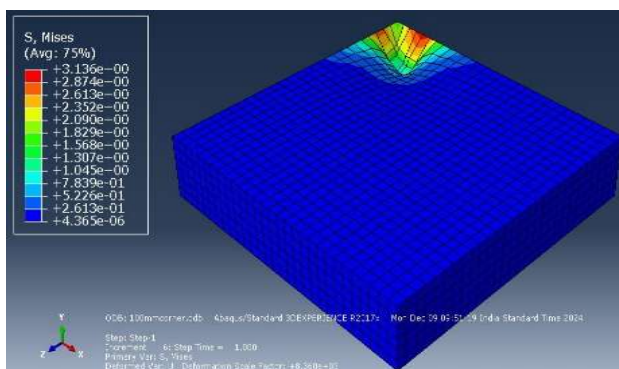


Figure 3: (c) Maximum critical corner stress for the 100 mm layer thickness of GPC UTWT.

The critical corner stress exhibited a reduction of 12.83% when the dimension increased from 80 mm to 90 mm, followed by a further decrease of 9.15% as the dimension increased from 90 mm to 100 mm. Overall, the 100 mm GPC layer exhibited the best performance, minimizing stress making it the optimal choice for enhanced load distribution and durability.

A (ii). Effect of ultra-thin white topping GPC layer thickness on Critical Edge stress

The simulations reveal that increasing the GPC thickness significantly reduces the maximum edge stress, enhancing the structural performance.

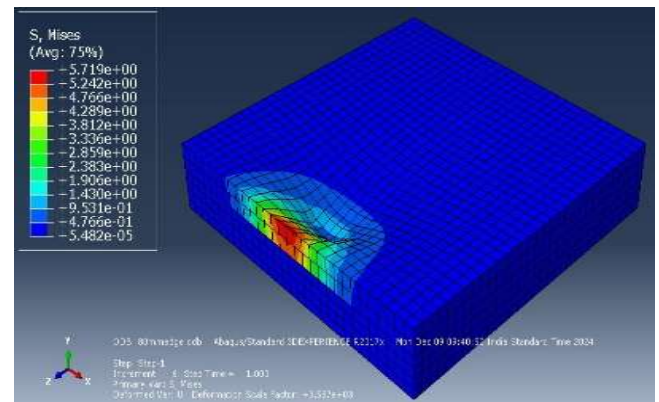


Figure 4: (a) Maximum Edge stress for the 80 mm layer thickness of GPC UTWT

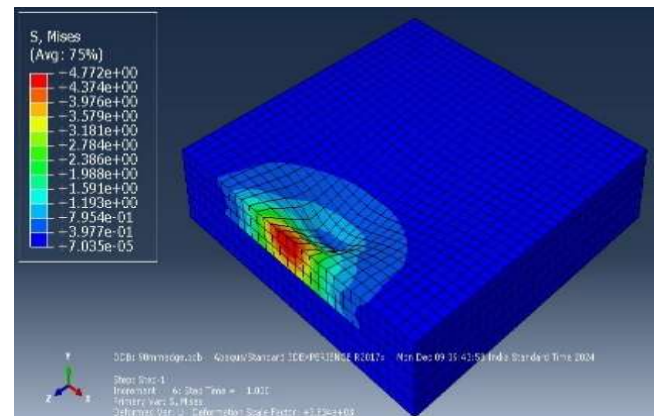


Figure 4: (b) Maximum Edge stress for the 90 mm layer thickness of GPC UTWT

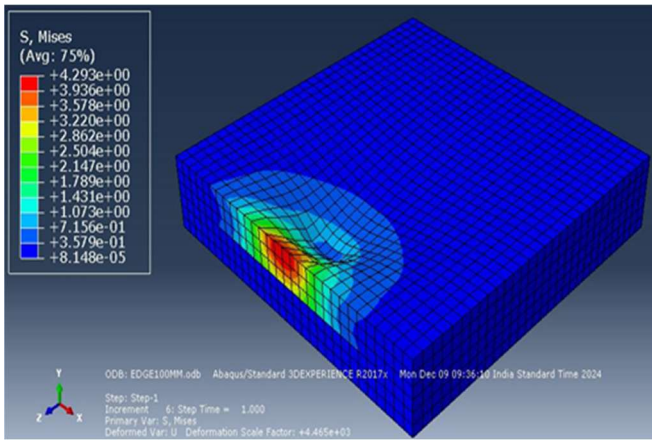


Figure 4: (c) Maximum Edge stress for the 100 mm layer thickness of GPC UTWT.

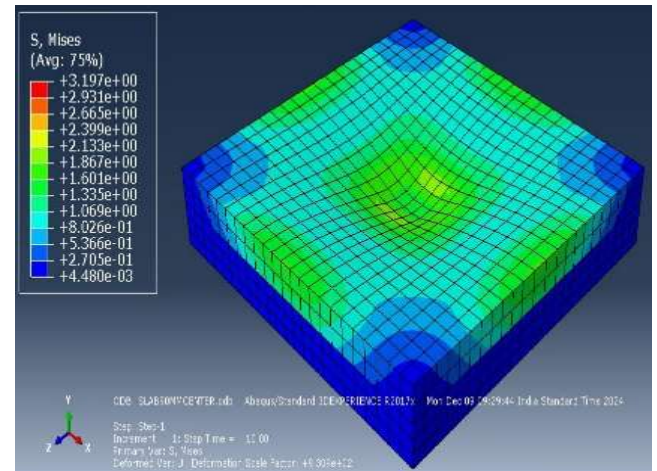


Figure 5: (b) Maximum Interior stress for the 90 mm layer thickness of GPC UTWT;

The results in Figure 4 showed that increasing the thickness of the GPC layer significantly reduced stress along the edges. The maximum edge stress for the 80 mm layer was 5.719 MPa, which was reduced to 16.54% for the 90 mm layer. This represents a total reduction of approximately 25% in maximum edge stress from the 80 mm to the 100 mm layer.

A (iii) Effect of ultra-thin white topping GPC layer thickness on Critical Interior stress

FEM models evaluate the effect of varying UTWT GPC layer thickness on critical interior stress shown in Figure 5. Increasing the thickness to 90 mm slightly increased the critical interior stress, to 2.37% compared to 80 mm slab due to stiffness variation. However, further increasing the thickness to 100 mm significantly reduced the stress, showing a 9.56% reduction relative to the 80 mm slab.

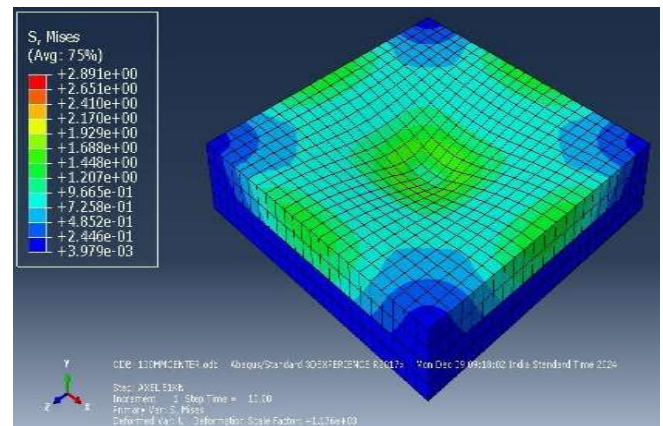


Figure 5: (c) Maximum Interior stress for the 100 mm layer thickness of GPC UTWT.

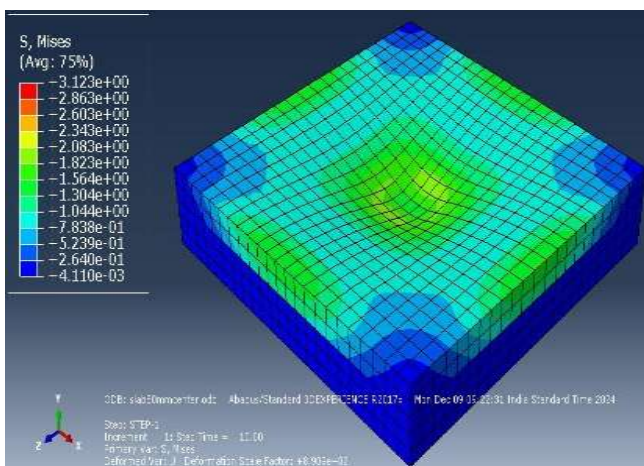


Figure 5: (a) Maximum Interior stress for the 80 mm layer thickness of GPC UTWT;

The stress contours showed better load distribution with increasing thickness, as higher stiffness effectively reduced stress concentrations near the loading point. These results demonstrate that a 100 mm GPC layer provides better structural resilience and impact resistance compared to thinner slabs.

B. Analytical Study on Interface Vertical and Horizontal Shear Stress

The interface between the GPC overlay and the asphalt concrete layer is critical for ensuring the structural performance of UTWT. The vertical and horizontal shear stresses at the interface directly increases the bonding strength and load transfer efficiency. Vertical force (τ_{max}) at the interface arises due to compressive strength transferred from the overlay to the asphalt layer (reference). Increasing the overlay thickness from 80 mm to 100 mm results in a

5.2% reduction exhibiting the lowest shear stress, making it more resilient against shear-induced failure.

Finite element models as shown in Figure 5 illustrate the distribution of positive shear stress at the interior positions. These analyses highlight the effect of overlay thickness on stress magnitudes and distributions under applied loading conditions. The stress concentration at 80mm geopolymer UTWT reflects higher sensitivity of thinner overlay to localized deformations. The shear stress at 90 mm UTWT is 4.27% higher than 80 mm overlay and the distribution is more uniform. The 100 mm GPC overlay exhibited the lowest shear stress among the three configurations with 11.44% reduction. This reduction in stress magnitude is attributed to higher stiffness and greater load distribution capacity provided by the thicker overlay. This further demonstrates enhanced resistance to deformation and localized stress peaks, making it more suitable for high-traffic applications.

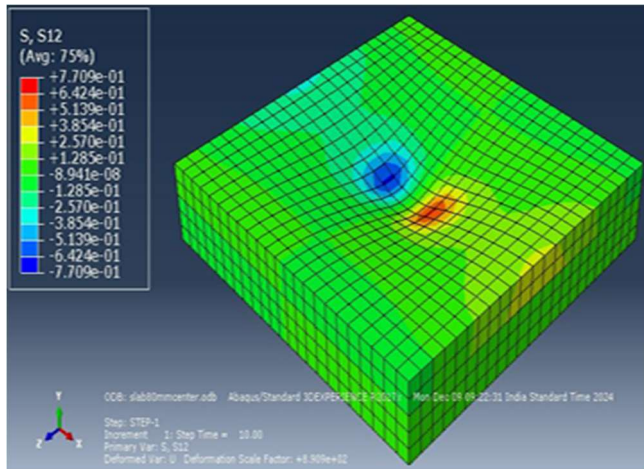


Figure 6(a): Maximum Vertical Shear Stress for the 80 mm layer thickness of GPC UTWT at Interior Loading condition.

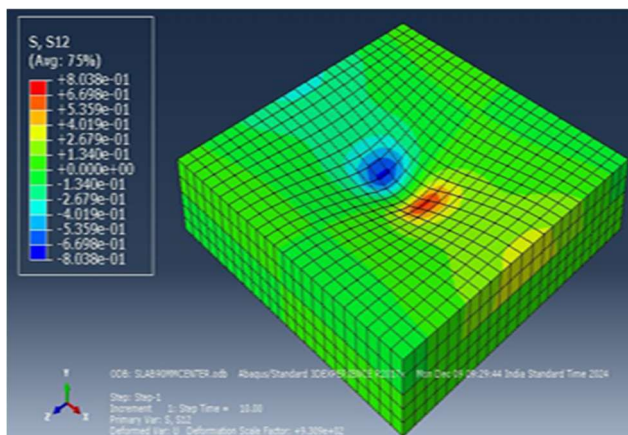


Figure 6(b): Maximum Vertical Shear Stress for the 90 mm layer thickness of GPC UTWT at Interior Loading condition.

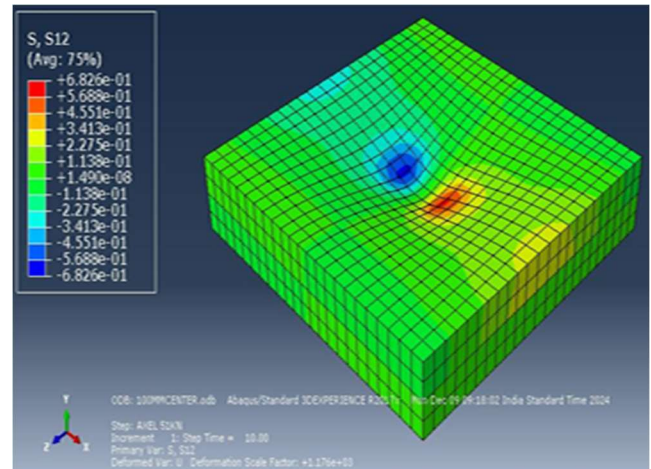


Figure 6 (c): Maximum Vertical Shear Stress for the 100 mm layer thickness of GPC UTWT at Interior Loading condition.

IV. RESULTS AND DISCUSSION

The results obtained from both analytical calculations and FEM simulations conducted in ABAQUS are compared. The analysis focused on stresses at critical positions – edge (σ_e), Corner (σ_c), and Interior (σ_i) for varying overlay thicknesses. Table 2 represents comparisons of critical stresses between analytical and FEM for 80 mm, 90 mm, and 100 mm GPC overlay thickness. For edge stresses, the percentage variation between analytical and FEM results ranged from 3.47% at 90 mm to 7.97% at 100 mm, demonstrating a relatively close agreement between the two approaches. The significance of employing FEM lies in its ability to accurately capture edge stress variations, particularly in thinner overlays where traditional analytical assumptions may underestimate stress intensities. FEM effectively predicts stress concentrations at pavement edges due to its finer mesh resolution and ability to account for slab rigidity effects (Wu et al., 2023). Thicker overlays, such as 90 mm, and 100 mm demonstrated improved performance in terms of stress dissipation, aligning closely with analytical predictions.

Corner stresses exhibited larger variations between analytical and FEM results at 90 mm overlay, suggesting that analytical methods under predict stress concentrations at corners due to simplified boundary assumptions. The 80 mm overlay showed a variation of 14.5%, while the 100 mm overlay had the lowest variation (12%). FEM approach demonstrated superior accuracy by identifying confined effects at the corners, whereas analytical approach provides plausible approximations in thicker overlays. The influence of thickness and interface bonding on overlay performance using 3D FEM revealed that FEM identifies stress amplifications near corners due to geometric discontinuities, while analytical approaches smooth out abrupt changes

(Dormohammadi et al., 2019). The interface bonding properties significantly influence stress concentrations at corner zones, particularly for thinner overlays, requiring FEM for localized stress evaluation (Barman et al., 2017).

Interior stresses show the lowest percentage variations for 90 mm and 80 mm overlay thicknesses, ranging from 8.51% to 15.26%, indicating better agreement between analytical and FEM results compared to edge and corner stresses. The 100 mm overlay exhibits a higher variation of 13.78%. The variations observed across all stress locations, edge, corner, and interior, highlight the fundamental differences between empirical approximations and numerical simulations. Analytical methods rely on simplified assumptions about load distribution and boundary effects, making them suitable for preliminary estimates. However, these methods tend to provide smoother stress predictions, potentially overlooking localised stress peaks captured by FEM, particularly at corners and edges. Increasing overlay thickness reduces stress magnitudes and percentage variations, demonstrating better load distribution and improved performance with thicker overlays. Thicker overlays (90 mm and 100 mm) align more closely with FEM results, validating their use for high-traffic pavements.

Table 2 Comparison of Results for stresses using the FEM and Westergaard's equation for different layers of UTWT thickness.

Loading Condition	Normal Stresses (MPa) @ Ea = 1600 MPa					
	ABAQUS			Analytical		
	80mm	90	100	80	90	100
	mm	mm	mm	mm	mm	mm
Corner	3.96	3.45	3.13	3.46	2.92	2.79
Edge	5.71	4.77	4.29	5.42	4.61	3.97
Interior	3.12	3.20	2.89	2.71	2.95	2.54

Figure 7: Logarithmic regression equation between corner stress and GPC overlay thickness

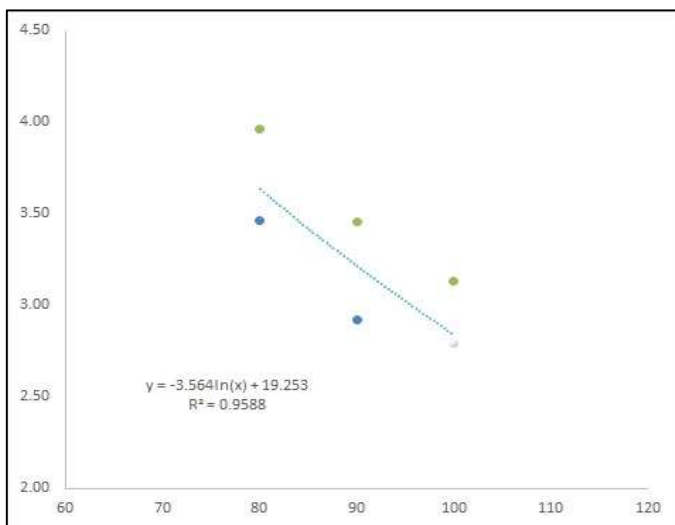
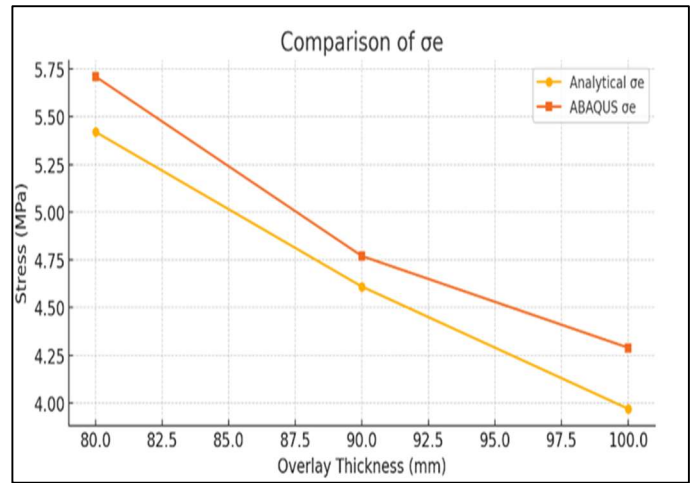


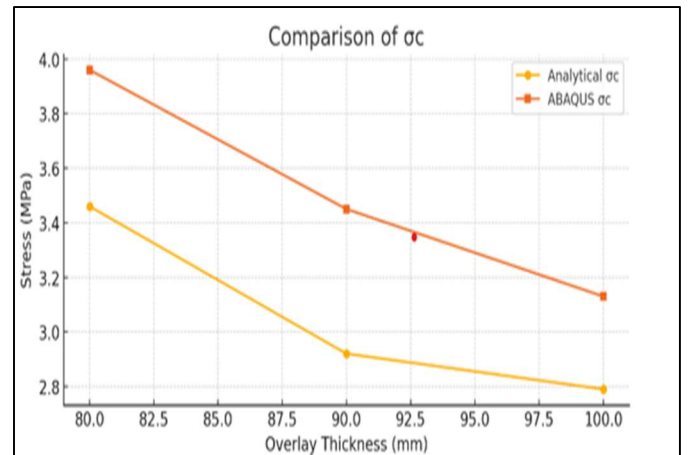
Figure 7 demonstrates the stress-thickness relationship and provides a mathematical model for predicting corner stress values based on layer thickness. The equation models a decreasing trend, showing that corner stress reduces as thickness increases.

The logarithmic regression equation (10) shows critical corner stress is given as:

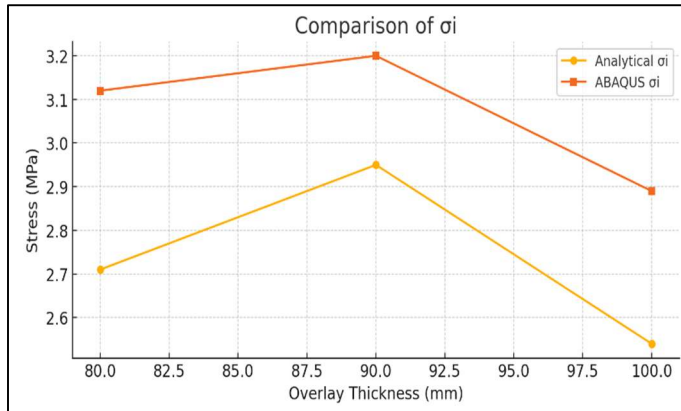
$$\sigma_c = -3.564 \ln(h_c) + 19.253 \tag{10}$$



(a)



(b)



(c)

Figure 8 (a),(b) & (c): Graph shows the comparison between stresses at critical locations (corner, edge, interior) and Overlay thickness of UTWT GPC.

Figures 8 a, b represents edge and corner stresses show a similar decreasing trend with increasing overlay thickness in both analytical and FEM results, indicating consistent behaviour. FEM captures boundary effects more accurately, reflecting localized interactions and stiffness transitions. However, the Figure 8c, the peak interior stress at 90 mm, the UTWT might be reaching a critical stiffness level to develop significant restraint at the interface with the asphalt layer.

Table 3 Comparison of Analytical and FEM Vertical Shear Stress

Overlay Thickness (mm)	Analytical (MPa)	FEM (MPa)
80	0.690	0.771
90	0.728	0.803
100	0.654	0.683

Table 3 shows a comparative evaluation of analytical and FEM results for interface vertical shear stress (τ_{max}) at different overlay thicknesses. The results indicate that FEM consistently predicts slightly higher stress values compared to analytical methods, particularly for thinner overlays. It can be observed analytically from Table 3 that increasing the modulus of the supporting layer to 1600 MPa or increasing the asphalt thickness from 80 mm to 100 mm results in minimal changes to shear stress values, with reductions of more than 5%. For instance, at 80 mm thickness, FEM recorded higher stresses due to its ability to capture localised stress concentrations, resulting in a 5.29% variation. As the overlay thickness increased to 90 mm, the variations increased by 4.15% at 90 mm and decreased by 11.41% at 100 mm. Overall, analytical

methods offer reasonable approximations for preliminary design calculations, particularly for interior stresses where load distribution tends to be more uniform. However, FEM simulations are more reliable for detailed analysis as they incorporate localised stress variations and material stiffness effects.

V. CONCLUSION

The study evaluated the structural behaviour of Geopolymer concrete UTWT on asphalt pavements using both Analytical and Finite Element Modelling in ABAQUS.

1. Increasing UTWT overlay thickness significantly reduces the critical corner, edge, and interior stresses. The 100 mm overlay thickness exhibited the lowest stresses, demonstrating better load distribution and higher structural capacity than thinner overlays.
2. Stress decreases logarithmically with increasing thickness, supporting the need for thicker layers to enhance structural performance.
3. Interface bonding conditions between the GPC overlay and asphalt layer were identified as critical factors influencing stress behaviour.
4. FEM simulations effectively captured stress concentrations at critical points, particularly at corners and edges which analytical models underestimated. FEM analysis is essential in pavement design, providing accurate predictions of structural response, optimizing performance, and reducing failure risk.
5. A reduction in geopolymer concrete slab thickness from 100 mm to 80 mm markedly amplifies the maximum shear stress in ultra-thin white topping (UTWT) systems.

VI. PRACTICAL IMPLICATIONS

Ultra-Thin Geopolymer Concrete Overlays can be effectively applied in low- to medium-volume roads, urban rehabilitation projects, bus lanes, and light-duty industrial pavements, where full-depth reconstruction is impractical or cost-prohibitive. The use of geopolymer materials reduces cement dependency, offering a more sustainable and environmentally friendly solution for pavement rehabilitation.

This approach addresses key challenges in traditional overlay systems, including:

- Premature failure due to insufficient structural capacity
- High CO₂ emissions from cement-based overlays
- Limited bonding with asphalt substrates.

VII. RECOMMENDATION:

- A minimum UTWT thickness of 100 mm is recommended for ensuring sufficient structural integrity under repeated traffic loading, particularly where shear stress is critical.
- Proper surface preparation and bonding techniques must be prioritized to prevent delamination and performance loss at the interface layer.
- Future work should explore FEM studies to include temperature variations and dynamic loading scenarios will further improve the reliability of design recommendations.

AUTHOR CONTRIBUTIONS

S Rayapudi : Conceptualization, Software, Validation, Writing – original draft, Methodology. **Dr. TC Rao**: Review & editing.

REFERENCES

- Barman, M., Vandebossche, J.M. & Li, Z., (2017).** Influence of interface bond on the performance of bonded concrete overlays on asphalt pavements. *Journal of Transportation Engineering, Part B: Pavements*, 143(3).
- Birmann, D., (1981).** *Influence of hydraulically bound base layers on the loading of concrete pavements: experimental and theoretical investigations with special consideration of edge loading.* Unpublished doctoral dissertation. TU München, Germany.
- Dormohammadi, A., Tandon, V. & Rodarte, A.A., (2019).** *Evaluating influence of thickness and interface bonding on overlay service life using 3D FEM.* *International Journal of Geomechanics*, 19(4).
- Honghui, L., Xiaojuan, L. & Yuan, L., (2020).** *Analysis of shear failure of asphalt pavement under horizontal force.* *DEStech Transactions on Environment, Energy and Earth Science*.
- Indian Roads Congress (IRC), (2008).** *IRC-SP-76: Guidelines for white topping on bituminous pavements.* New Delhi: IRC.
- Ioannides, A.M., Davis, C.M. & Weber, C.M., (1999).** *Westergaard Curling Solution Reconsidered.* *Transportation Research Record*, 1684(1), pp.61–70.
- Jiao, L., Wu, R. & Harvey, J., (2023).** *Reflective crack initiation of asphalt overlays on jointed concrete pavement using finite element model.* *International Journal of Pavement Engineering*, 24(2), p.2154350.
- Juhasz, I. & Eng, D., (2015).** *Performance of bonded concrete overlays on asphalt pavements in Alberta, Canada.* *Journal of Infrastructure Engineering*.
- Jundhare, D.R. & Khare, K.C., (2013).** *Life cycle cost analysis of bituminous and concrete pavements.* *International Journal of Pavement Research and Technology*, 6(3), pp.128–133.
- Krishna, U.S.R. & Ch, N.S.K., (2023).** *Analytical modelling of ultra-thin white topping cement concrete overlay on bituminous concrete pavement using ANSYS.* *World Journal of Engineering*, 20(4), pp.690–703.
- Mack, J.W., Wu, C.L., Tarr, S.M. & Refai, T., (1997).** *Model Development and Interim Design Procedure Guidelines for Ultra-Thin White Topping Pavements.* In: *Proceedings of the 6th International Conference on Concrete Pavement Design and Materials for High Performance.* Purdue University, West Lafayette, IN, 1, pp.231–256.
- Mampearachchi, W.K., (2012).** *Feasibility of whitetopping pavements for resurfacing thin asphalt pavements.* *Journal of the National Science Foundation*.
- Ministry of Road Transport & Highways (MoRTH), (2001).** *Specifications for road and bridge works.* New Delhi: Government of India.
- Mu, B. & Vandebossche, J.M., (2007).** *Cohesive zone model for asphalt-concrete interface analysis in white topping overlays.* *International Journal of Pavement Engineering*, 8(3), pp.178–185.
- NguyenDinh, N., (2023).** *Interface horizontal shear strength requirement in ultra-thin white topping (UTW) pavement.* *IOP Conference Series: Materials Science and Engineering*, 1289.
- Nishiyama, T., Lee, H. (David) & Bhatti, M.A., (2005).** *Investigation of Bonding Condition in Concrete Overlay by Laboratory Testing, Finite Element Modeling, and Field Evaluation.* *Transportation Research Record*, 1933(1), pp.15–23.
- Olita, S., Diomedi, M. & Ciampa, D., (2020).** *Alternative formula for rigid pavement stress calculation in corner load conditions.* *The Baltic Journal of Road and Bridge Engineering*, 15(5), pp.59–79.
- Rashad, A.M., (2015).** *An investigation of high-volume fly ash concrete blended with slag subjected to elevated temperatures.* *Journal of Cleaner Production*, 93(Supplement C), pp.47–55.
- Rashmi, S., Kumar, R., Akki, B. & Reddy, R., (2020).** *Performance studies on white topping layers over flexible pavement.* *IOP Conference Series: Materials Science and Engineering*, 981.
- Rasmussen, R.O. & Rozycki, J., (2004).** *Overview of ultra-thin white topping applications in the United States.* *Transportation Research Record*.
- Rayapudi, S. & Rao, T.C.S., (2024).** *Strength characteristics and impact resistance of fiber-reinforced geopolymer concrete elements.* In: *Low Carbon Materials and Technologies for a Sustainable and Resilient Infrastructure.* Singapore: Springer.

- Thomas, M., (2013).** *Supplementary Cementing Materials in Concrete*. 1st ed. CRC Press.
- Turner, L.K. & Collins, F.G., (2013).** *Carbon dioxide equivalent (CO₂-e) emissions: A comparison between geopolymer and OPC cement concrete*. *Construction and Building Materials*, 43, pp.125–130.
- Vandenbossche, J.M., (2017).** *Predictive structural model for bonded concrete overlays on flexible pavements*. *Journal of the Transportation Research Board*.
- Zhu, M. & Weng, X., (2019).** *Three-dimensional FEM loading stress analysis on a new airport concrete pavement ultra-thin whitetopping overlay structure*. *Structural Concrete*, 20(1), pp.80–89.